# A water wave analog of the Casimir effect

Bruce C. Denardo,[a] Joshua J. Puda, and Andrés Larraza
*Department of Physics, Naval Postgraduate School, Monterey, California 93943*

(Received 28 October 2008; accepted 3 August 2009)

Two rigid plates are vertically suspended by thread such that they are parallel to and opposite each other. The plates are partially submerged in a dish of liquid that is attached to the top of a vertical shake table. When the shake table is driven with noise in a frequency band, random surface waves are parametrically excited, and the plates move toward each other. The reason for this attraction is that the waves carry momentum, and the wave motion between the plates is visibly reduced. The behavior is analogous to the Casimir effect, in which two conducting uncharged parallel plates attract each other due to the zero-point spectrum of electromagnetic radiation. The water wave analog can be readily demonstrated and offers a visual demonstration of a Casimir-type effect. Measurements of the force agree with the water wave theory even at large wave amplitudes, where the theory is expected to break down. The water wave analog applies to side-by-side ships in a rough sea and is distinct from the significant attraction that can be caused by a strong swell.
[DOI: 10.1119/1.3211416]

## I. INTRODUCTION

In the Casimir effect two conducting uncharged parallel plates attract each other due to the ground state or "zero-point" spectrum of electromagnetic radiation at zero absolute temperature.[1] The effect can be understood and calculated as an imbalance in the radiation force on the inside and the outside surfaces of the plates.[2] A radiation force on a body is the time-averaged force due to waves that are incident on the body. The force arises due to the momentum of the waves and is proportional to the energy density. For the electromagnetic zero-point spectrum the ground state energy of $\hbar\omega/2$ for each normal mode leads to the classical spectral energy density (energy per unit frequency per unit volume) $\hbar\omega^3/2\pi^2c^3$ in empty space, where $\hbar$ is the reduced Planck's constant, $\omega$ is the angular frequency, and $c$ is the speed of light. Although this energy cannot be directly observed, the presence of the plates discretizes the spectrum between and transverse to the plates, which causes the imbalance of the radiation force. The energy density (the integral of the spectral energy density over frequency) is infinite, and thus the force on either side of a plate is infinite. The use of a regularization procedure[2,3] yields the net attractive force per unit area of $\pi^2\hbar c/240d^4$, where $d$ is the distance between the plates.

The Casimir effect is not restricted to photons but is expected to occur for any waves that carry momentum. For example, two rigid conducting uncharged parallel plates that are vertically and partially submerged in liquid helium are expected to attract each other not only due to zero-point photons but also due to zero-point phonons (acoustic excitations) and zero-point ripplons (liquid surface wave excitations). To our knowledge, this effect has not yet been observed.

Analog
Casimir effects are similarly not restricted. By analog we mean that the force between bodies arises from driven waves rather than a zero-point spectrum. Analog Casimir effects have been investigated for two side-by-side ships in a strong swell (long-wavelength waves),[4] acoustic waves,[5,6] two beads on a vibrating string,[7] and other systems.[8] As in the Casimir effect, the behavior in these driven systems can be understood and calculated as an imbalance in the radiation force.

In this paper we investigate an analog Casimir effect in which two rigid parallel plates are vertically suspended and partially submerged in a dish of liquid (Fig. 1). The dish is attached to the top of a vertical shake table that is driven with noise in a finite band of frequencies. Random surface waves are parametrically excited, and the plates are observed to move toward each other as a result of the waves. The longest wavelength in the spectral band is sufficiently small compared to the size of the dish so that the waves are approximately homogeneous and isotropic outside the plates (see Fig. 1). We are primarily interested in the simple case in which the plate separation distance is sufficiently small so that the wave motion is negligible between and transverse to the plates, as shown in Fig. 1, which can occur because a smallest wavelength exists in the dish. This situation yields an attractive force that is independent of the distance and is proportional to the energy density and thus the mean-square amplitude of the waves.

The analogy of our water wave system to the Casimir effect is not exact. Because the water waves are driven, the energy density of the spectrum is not infinite, so a regularization procedure is not needed. Furthermore, we are primarily concerned with the case of closely spaced plates, which yields a force that is independent of the separation distance $d$. This behavior is in contrast to the Casimir force, which has a $1/d^4$ dependence due to the divergence of the $\omega^3$ spectrum at high frequencies.

An example of an analog Casimir system that is similar, in principle, to our water wave system is two conducting parallel plates in a microwave cavity, where the microwave radiation is driven in a finite band of frequencies. The maximum wavelength should be small compared to the size of the cavity so that the electromagnetic field is approximately homogeneous and isotropic. As in the water wave case, a sufficiently small plate separation distance yields an attractive force that is independent of the distance and is proportional to the mean-square amplitude of the waves. The microwave force can be easily estimated. The radiation pressure due to homogeneous and isotropic electromagnetic waves incident upon a perfectly reflecting surface is $I/3c$,[9] where $I$ is the average intensity $\epsilon_0 E_{\text{rms}}^2$, $\epsilon_0$ is the vacuum permittivity, and $E_{\text{rms}}$ is the root-mean-square electric field. The attractive force per unit area for closely spaced plates with a negligible

(a)

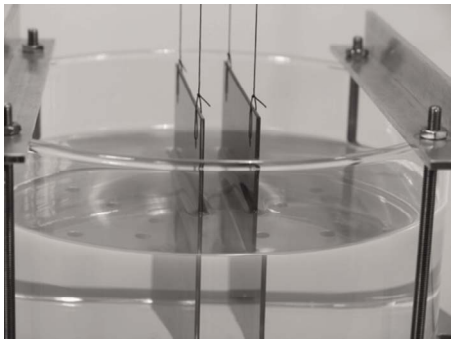

(b)

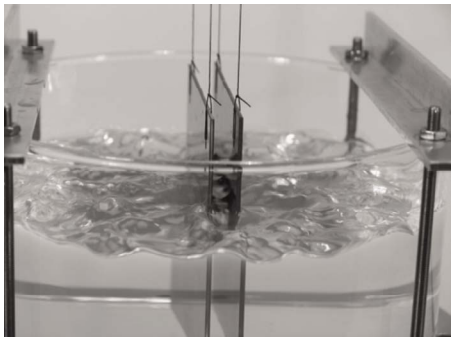

(c)

Fig. 1. Apparatus for demonstrating a water wave analog of the Casimir effect. (a) Support arrangement for the plates with thread and pendulum clamps. The thread length is 80 cm. (b) Parallel plates partially but deeply submerged in ethyl alcohol with the fluorescein dye. The dish has the diameter of 19 cm and is attached to a vertical shake table. (c) Shaker produces waves that cause a substantial attraction of the plates. There is very little wave motion between the plates.

field between the plates is thus $\epsilon_0 E_{\mathrm{rms}}^2/3c$. The electric field due to a magnetron in a microwave oven is limited by the dielectric breakdown strength of air, which is $3\times10^6$ V/m. For two $10\times10$ cm$^2$ closely spaced plates, this field yields a force that has a mass equivalent of the order of 1 $\mu$g, which is four orders of magnitude smaller than the order-of-magnitude value of 10 mg in our water wave experiment. To our knowledge, the microwave analog Casimir effect has not yet been observed.

Our water wave analog has application to two side-by-side ships in a rough sea and is distinct from the effect due to a swell.[4] Due to its long wavelength, the swell causes the ships to roll side-to-side in phase. This motion generates secondary waves outside the ships. Between the ships, however, the waves are 180° out-of-phase and thus tend to cancel. A wave propulsion effect consequently occurs in which either ship drives itself toward the other due to the emission of waves. As shown in Ref. 4, this attraction can be significant.

Casimir forces can be repulsive in zero-point[10] and analog cases. When the band of waves has a nonzero lower frequency limit, which often occurs in analog Casimir effects, a repulsive force can occur between two parallel plates for some separation distances. This force has been calculated and observed in the acoustics case.[5]

Our water wave system offers a visual demonstration of an analog Casimir effect. All three aspects are directly observed: The generation of waves, a substantial reduction in wave motion between the plates, and the attraction of the plates. We describe the demonstration in Sec. II. Gravity-capillary waves are discussed in Sec. III, and the theory of the radiation force due to random gravity waves is developed in Sec. IV, where we also estimate the attractive force between two side-by-side ships in a rough sea. The theory assumes linear (sinusoidal) waves, whereas the waves in the demonstration can be noticeably nonlinear, so the validity of the theory is questionable in this case. In addition, other effects could be playing a role in the observed attraction. Accordingly, we describe a quantitative experiment in Secs. V and VI and compare the data to the theory. Concluding remarks are made in Sec. VII.

## II. DEMONSTRATION

It is not difficult to produce a demonstration of the water wave analog of the Casimir effect (Fig. 1). We have arranged the entire apparatus to be on a table that was rolled into a classroom. We use 9.5 cm square acrylic or PVC plates with a thickness of 1.6 mm. Each plate is suspended with two 80 cm lengths of thread whose upper ends are secured by clamps. As shown in Fig. 1(a), opposing pendulum clamps[11] are very convenient for the purpose of the suspension. The clamps are attached to a common horizontal support rod that is held by two vertical rods which are clamped to the table. The plates are separated by approximately 1.7 cm in equilibrium (in the absence of wave motion).

We use a glass dish with diameter of 19 cm and height of 10 cm as a container.[12] The dish is filled to a depth of 7 cm with ethyl alcohol or water, and a small amount of the fluorescein dye is added so that the liquid is easily observable. The dish rests on a vertical shake table that produces waves. We use a commercial shaker,[13] but a loudspeaker can be adapted for this purpose.[14] We attach the dish to the shaker because the acceleration amplitude of the shaker can exceed the acceleration due to gravity for the generation of higher-amplitude waves. As shown in Fig. 1(b), the plates are partially but deeply submerged (approximately 2/3 of a plate). The deep placement serves two purposes: To prevent the wave motion from passing under the plates and into the region between the plates and to increase the viscous damping to reduce the motion of the plates due to fluctuations of the random waves.

The shaker causes the effective acceleration due to gravity to be modulated in the frame of reference of the dish, which parametrically excites surface waves. A similar excitation can occur for a pendulum whose pivot is vertically oscillated.[15] To produce random waves, we drive the shaker with noise from a function generator that is bandpass filtered[16] in the octave band of 10–20 Hz and then power

amplified. The waves cause the plates to be displaced toward each other, as shown in Fig. 1(c). As explained in Sec. I, this attraction occurs because the waves carry momentum, and the wave motion between the plates is substantially reduced, which is clearly visible. The waves are strongly nonlinear at greater drive amplitudes, as evidenced by liquid droplets that are occasionally ejected from the dish. For a sufficiently large drive amplitude of the shaker, the plates eventually touch, after which surface tension causes them to stick together. The demonstration can be repeated with the plates far apart (6 cm is appropriate). No attraction is observed, which is consistent with the wave motion between the plates having the same appearance as the wave motion outside.

Ethyl alcohol yields a noticeably greater force than water, which is an important advantage because the force is weak. Although we initially performed the demonstration with water, we now only use ethyl alcohol. The greater force of alcohol is surprising because the smaller density yields less momentum and thus less force for a fixed wave amplitude. Moreover, the drive displacement amplitude for our shaker is the same for alcohol and water, and the kinematic viscosity of alcohol is greater, so the wave response of alcohol is expected to be less. However, what is relevant is the *quality factor* of the surface wave modes, and alcohol yields a greater quality factor due to the substantial wetting of the wall and plates whether or not a wetting agent is added to water. The greater quality factor of alcohol is especially important for parametric excitation because there is a dissipation-dependent drive amplitude threshold for any response to occur.[15]

There are several reasons for our choice of driving in the frequency band of 10–20 Hz. Lower bands require a higher amplitude of the shaker for waves to be excited, and the response consists of intermittent slowly varying high-amplitude standing waves which can cause the plates to stick together. Bands higher than 10–20 Hz produce violent standing waves in the threads, which cause substantial motion of the plates. Attraction of the plates is still observed, however. Intermittent small-amplitude standing waves in the threads occur in the 10–20 Hz band but have a negligible effect on the plates.

## III. GRAVITY-CAPILLARY WAVES

For sufficiently large wavelengths, where gravity is the dominant restoring force, waves on the surface of a liquid are called gravity waves. For sufficiently small wavelengths, where surface tension dominates, the waves are called capillary waves. A linear (small-amplitude) deep gravity-capillary wave of frequency $f$ and wavelength $\lambda$ has the dispersion relation[17]

$$\omega^2 = gk + \frac{\gamma}{\rho}k^3, \tag{1}$$

where $\omega = 2\pi f$ is the angular frequency, $k = 2\pi/\lambda$ is the wave number, $g$ is the acceleration due to gravity, $\gamma$ is the surface tension coefficient of the liquid, and $\rho$ is the density. The amplitude of the particle motion due to a wave decreases exponentially with depth, where the exponential coefficient equals the wave number $k$, and thus the liquid is "deep" as long as the depth exceeds only about a wavelength.

At 20 °C and atmospheric pressure, the density of water is $\rho = 0.998$ g/cm$^3$ and the surface tension coefficient is $\gamma = 72.8$ dynes/cm; ethyl alcohol has $\rho = 0.791$ g/cm$^3$ and $\gamma = 22.3$ dynes/cm. Figure 2 shows a graph of the dispersion relation in Eq. (1) for ethyl alcohol (solid curve) and water (dashed curve) for $g = 981$ cm/s$^2$. The dotted line corresponds to pure gravity waves ($\gamma = 0$), whose dispersion relation is independent of the properties of the liquid.

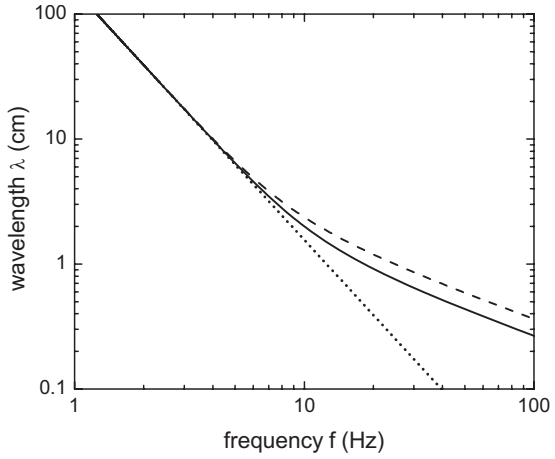


Fig. 2. Wavelength as a function of frequency according to the dispersion relation (1) for deep gravity-capillary waves on ethyl alcohol (solid curve) and water (dashed curve), and for pure deep gravity waves (dotted line).

Gravity and surface tension contribute equally to the restoring force at the crossover wave number $k_c$, which is found by equating the two terms on the right side of Eq. (1), yielding $k_c = \sqrt{\rho g/\gamma}$. The crossover frequency and wavelength are

$$f_c = \frac{1}{\pi}\left(\frac{\rho g^3}{4\gamma}\right)^{1/4} \quad \text{and} \quad \lambda_c = 2\pi\sqrt{\frac{\gamma}{\rho g}}. \tag{2}$$

The crossover values are $f_c = 13.5$ Hz and $\lambda_c = 1.71$ cm for water and $f_c = 17.1$ Hz and $\lambda_c = 1.07$ cm for ethyl alcohol.

In the demonstration and the experiment (see Secs. V and VI) we drive the shake table in a band of noise from 10 to 20 Hz. Because the drive is parametric, the primary response of the waves is half of the drive frequency range,[15] from 5 to 10 Hz, which we have confirmed by measurement (see Sec. VI). The relatively large crossover frequency of 17.1 Hz for ethyl alcohol and the closeness of ethyl alcohol gravity-capillary curve and gravity wave line at 10 Hz in Fig. 2 suggest that it is reasonable to approximate the motion as pure gravity waves for comparing theory to experimental data. The fact that the approximation is better for ethyl alcohol than water is one of the advantages of the use of ethyl alcohol, in addition to the advantages cited in Sec. II.

## IV. THEORY OF THE RADIATION FORCE DUE TO RANDOM GRAVITY WAVES

It might be thought that the momentum of a traveling wave averages to zero. A closer inspection reveals a small asymmetry that leads to a nonzero net momentum. For sound, the particle velocity in a compression is in the direction of propagation of the wave, while the particle velocity in an expansion is in the opposite direction. The average particle velocity vanishes, but there is a net momentum in the direction of the wave because the density is greater in the compression. This momentum is small (second order in the

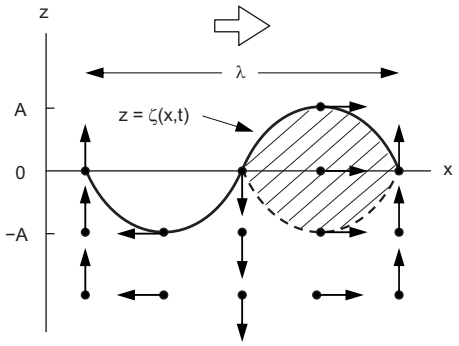


Fig. 3. Representation of a small-amplitude ($A \ll \lambda$) deep gravity wave traveling in the positive $x$ direction. The particle motion is circular; the bold arrows represent instantaneous particle velocity. The net momentum over one wavelength is the positive amount in the hatched region.

amplitude of the wave) because it reduces to the integral of the product of the particle velocity and the change in the density, both of which are first order. The momentum can be demonstrated by the rotation of an acoustic radiometer in a homogeneous and isotropic noise field.[9]

An analogous asymmetry occurs for water waves. Consider one wavelength of a small-amplitude deep gravity traveling wave (Fig. 3), where $x$ is the horizontal coordinate in the direction of propagation and $z$ is the vertical coordinate, with $z=0$ corresponding to the surface in equilibrium. The vertical displacement of the surface is $z=\zeta(x,t)$. The particle motion is circular;[17] the bold arrows in Fig. 3 represent the instantaneous particle velocity. The net vertical momentum vanishes by symmetry. The negative horizontal momentum below the negative hump cancels the positive horizontal momentum below the dashed curve under the positive hump. Hence, over one wavelength the net momentum per unit length transverse to the wave is the positive amount in the hatched region. We next calculate this momentum to leading order in the amplitude of the wave.

The momentum per unit volume is the product of the density (which is uniform) and the particle velocity: $\rho \boldsymbol{u}$. To determine the average momentum $P$ per unit horizontal area, we first integrate the $x$ momentum per unit volume $\rho u_x(x,z,t)$ with respect to $z$ from $-\zeta$ to $\zeta$, or double the integral from 0 to $\zeta$ (refer to the hatched region in Fig. 3). We then integrate with respect to $x$ over the half-wavelength and divide by the wavelength. Because $u_x(x,z,t)$ and $\zeta(x,t)$ are both first-order quantities, $P$ is second order. The variation in $u_x$ with $z$ produces higher-order terms, and we set $u_x=u_x(x,0,t)$ for $P$ to be accurate to leading order. The result is that the average momentum per unit horizontal area is

$$P=\frac{2\rho}{\lambda}\int_{x=0}^{\lambda/2} u_x(x,0,t)\zeta(x,t)dx. \tag{3}$$

We now use some basic results from the linear theory of deep gravity waves.[17] A traveling plane wave of definite frequency has surface displacement $\zeta(x,t)=A\sin(\omega t-kx)$, where $A$ is the peak amplitude of the wave (Fig. 3). The particle velocity is $\boldsymbol{u}=\boldsymbol{\nabla}\phi$, where the velocity potential is $\phi(x,z,t)=c_pA\cos(\omega t-kx)$ and the phase velocity is $c_p=\omega/k$. If we substitute $\zeta(x,t)=A\sin(\omega t-kx)$ and $u_x=c_pkA\sin(\omega t-kx)$ into Eq. (3) and perform the integration, we obtain $P=\rho\omega A^2/2$. This momentum must move with the group velocity $c_g=d\omega/dk$, which is $c_g=c_p/2$ according to the dispersion relation (1) with $\gamma=0$. The average momentum flux density (per unit time per unit transverse length) is thus $S=c_gP=\rho gA^2/4$.

It is useful to cast the result for $S$ in terms of the average energy density (per unit horizontal area) $E$, which is readily shown to be twice the average potential energy density and is thus $E=\rho gA^2/2=2S$. For convenience, we use the root-mean-square vertical displacement amplitude $A_{\rm rms}=A/\sqrt{2}$ instead of the peak amplitude $A$ of the wave. The average momentum flux density (per unit transverse length) is then

$$S=\tfrac{1}{2}E=\tfrac{1}{2}\rho gA_{\rm rms}^2. \tag{4}$$

Whitham[18] calculated the momentum flux density for arbitrary depth using a Lagrangian method. This situation is complicated by a mean flow that occurs due to the finite depth. Whitham's results in the limit of infinite depth yields our result $S=E/2$ in Eq. (4).

We now determine the radiation force due to random deep gravity waves incident on one side of a fixed rigid vertical plate. The waves are assumed to be homogeneous and isotropic with average spectral energy density $E_\omega=dE/d\omega$. We also assume that the plate is sufficiently deep so that it is subject to essentially all of the wave motion, and the width of the plate is significantly greater than the largest wavelength so that geometrical wave theory applies. By Newton's second law, the radiation force due to waves that are normally incident upon the plate equals twice the average momentum flux density (4) multiplied by the horizontal width $a$ of the plate; the doubling is due to the perfect reflectivity. For the angle of incidence $\theta$ the force is reduced by the factor $\cos^2\theta$, which is due to the tensor character of the radiation stress. The reason is that one factor of $\cos\theta$ arises from the momentum being spread over a length greater than the cross-sectional length of a wave; the other factor arises from projecting the momentum perpendicular to the plate. The radiation force due to waves with frequencies between $\omega$ and $\omega+d\omega$ and angles between $\theta$ and $\theta+d\theta$ is thus $dF=aE_\omega\cos^2(\theta)d\omega d\theta/2\pi$, where the factor of $2\pi$ accounts for the force per unit angle for isotropic waves. Integration over frequency and angle (from $\theta=-\pi/2$ to $\pi/2$) yields the total radiation force

$$F=\frac{1}{4}\rho ga\int A_\omega^2 d\omega=\frac{1}{4}\rho gaA_{\rm rms}^2, \tag{5}$$

where we have used Eq. (4), and $A_{\rm rms}^2(\omega)=dA_{\rm rms}^2/d\omega$ is the spectral mean-square amplitude of the waves.

Two parallel plates with negligible wave motion between them will be attracted with the force (5). As an application, we consider two side-by-side ships in a rough sea. For historic clipper ships, Boersma[4] estimated that a strong swell causes an attractive force of $2\times10^3$ N, which is consistent with observations that the effect was dangerous but that sailors were able to tow a ship to safety. We assume a ship length of $a=20$ m and negligible wave motion between the ships. For a root-mean-square wave amplitude of $A_{\rm rms}=1$ m, the force of attraction according to Eq. (5) is approximately $F=5\times10^4$ N, which is a factor of 25 greater than the force due to the swell. For a root-mean-square amplitude of only 20 cm, the force is approximately the same as a strong swell. However, not all wavelengths contribute to the effect we have calculated. For wavelengths that are significantly

longer than the depth of the ships and significantly less than the separation distance, the wave motion between the ships will be approximately the same as the wave motion outside. Only the intermediate wavelengths contribute to the force.

## V. EXPERIMENTAL APPARATUS

The goal of our experiment is to ascertain whether the observed displacement of the plates is in quantitative agreement with the theory given in Sec. IV. For reasons discussed in Secs. II and III, we use ethyl alcohol rather than water. The demonstration apparatus discussed in Sec. II is employed, with the exception that we isolate the plate support rods from the shaker by using heavy-duty floor stands with extensions. This arrangement reduces vibrations of the threads and allows us to use longer lengths to increase the sensitivity of the plate displacements (see the following). The length of the threads is 1.0 m.

A plate suspended by threads forms a pendulum. Experimental values of the radiation force can be determined from measurements of the displacement of the pendulum. Because the length of the threads is large compared to the size of a plate, and the mass of the threads is small compared to the mass of a plate, it can be shown that the pendulum is simple to a good approximation. For small displacements of a plate from the vertical equilibrium state, the magnitudes of the horizontal force $F$ and the horizontal displacement $x$ are related by

$$F = \frac{mg}{L}x, \tag{6}$$

where we take $L$ to be the distance from the support to the top of a plate because the plates remain approximately vertical in the experiment. Buoyancy must be taken into account. The mass in Eq. (6) has the effective value $m=m_0 - \rho V$, where $m_0$ is the plate mass, $\rho$ is the density of the liquid, and $V$ is the submerged volume of a plate. Note that the pendulum sensitivity (displacement per unit force) is proportional to the length $L$ and inversely proportional to the mass $m$. Because the radiation force is small (see Sec. VI), a large length and small mass are desirable.

We measure the displacements of the plates by analyzing pictures taken with a high-resolution digital camera. A steel rule is rigidly supported just in front of the threads near the plates. By "zooming in" when we examine a picture, we can precisely determine the distance from a thread at one plate to a thread at the other plate. The displacement $x$ of a plate is then one-half of the difference of the equilibrium separation (with no waves) and the separation with waves. The equilibrium separation is approximately 1.7 cm.

We measure the wave motion with a hand-made two-wire AC resistive probe in a simple circuit with a series resistance $R_s$ (see Fig. 4).[19] (DC operation causes chemical reactions that lead to substantial drifts in the resistance.) We made the probe by baring the ends of two standard RG-58 coaxial cables, tying the two cables together, and grounding the shields. The wires have a diameter of 0.84 mm and are spaced 2.7 mm between their centers. The probe is securely attached to the assembly that anchors the dish to the shaker so that the probe is at rest relative to the dish. The function generator in the circuit in Fig. 4 supplies a carrier whose frequency is much greater than the frequencies of the waves. The voltage across $R_s$ is preamplified and sent to a lock-in amplifier[20] that demodulates the signal (that is, removes the carrier). Ethyl alcohol is very weakly conductive. The fluorescein has the added benefit of increasing the conductivity of the solution by two to three orders of magnitude, which substantially reduces unwanted electrical pick-up. The resistance $R$ of the solution is inversely proportional to the depth of the probe. We choose $R_s \ll R$ so that the voltage across $R_s$ is proportional to the depth. The probe is thus linear. Static measurements are performed to establish the linearity and to calibrate the probe. For the parameters in Fig. 4 the typical value of the sensitivity of our probe (as detected by the lock-in amplifier) is approximately 12 mV/mm. To measure the surface motion, we AC couple the output of the lock-in amplifier to a fast-Fourier transform (FFT) signal analyzer.

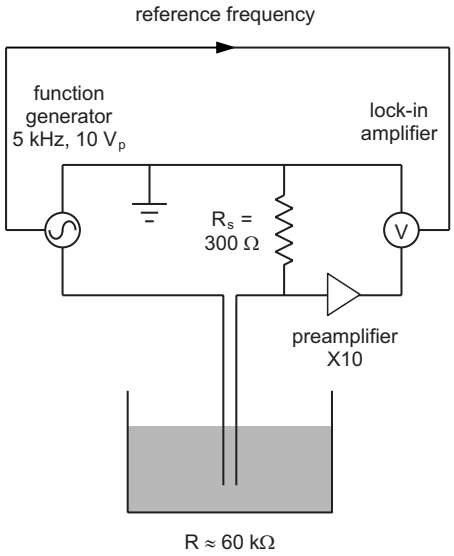


Fig. 4. Diagram of a probe system that measures the vertical displacement of waves on ethyl alcohol with fluorescein dye. Calibration is done statically by vertically incrementing the position of the probe wires. Waves are measured by feeding the output of the lock-in amplifier into a signal analyzer.

Although the parametric drive is a convenient source of the waves, it has the disadvantage of causing relatively large fluctuations of the wave amplitude due to modes continually growing to large amplitudes and then decaying. As a consequence, the plate separation distance also varies substantially. This behavior is due to a combination of a noise drive, a parametric drive amplitude threshold for excitation, and exponential growth above this threshold.[15] To obtain mean values of the root-mean-square wave amplitude and plate separation distance with standard deviations of the mean that are not large, we perform many measurements of these quantities (25 pictures and 15 or 22 FFT spectra). The measurements are also performed over the same time period, which is 2 or 3 min for each drive amplitude.

## VI. EXPERIMENTAL RESULTS

Figure 5 shows a typical surface wave spectrum from the two-wire probe. The primary response is in the band of 6–10 Hz, which is approximately half of the drive frequency range of 10–20 Hz and is thus in accord with the principal parametric resonance.[15] Figure 6 shows experimental data for the equivalent mass $F/g$ of the radiation force on a plate versus the mean-square amplitude $A_{\mathrm{rms}}^2$ of the waves. The values of $F/g$ are determined from Eq. (6) and measurements of the

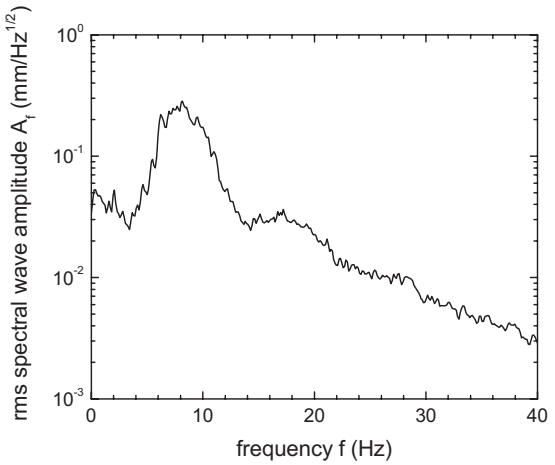


Fig. 5. Typical surface wave spectrum from the two-wire probe in Fig. 4. The root-mean-square surface wave vertical displacement is $A_{rms}=1.0$ mm, which corresponds to the midrange of the experiment (see Fig. 6).

plate displacement $x$. The solid line in Fig. 6 is the gravity wave theory, where we assume negligible wave motion between the plates in accord with our visual observations. Equation (5) then predicts a linear relation with slope $\rho a/4$, where $a$ is the horizontal width of a plate. The experimental data and theory approximately agree, although a systematic deviation is apparent—the data tend to lie above (or to the left of) the line. The deviation could be due to the theory being valid only to second order; specifically, sinusoidal waves are assumed. A breakdown of the theory is expected in our case because the wave motion at higher amplitudes is so strong that drops of liquid are occasionally ejected. However, if the theory breaks down, experiment and theory would show good agreement at smaller wave amplitudes, and an increasing fractional deviation as the amplitude increases. This behavior is not seen in the data in Fig. 6, so a breakdown due to the second-order accuracy of the theory is unlikely to be responsible for the deviation.

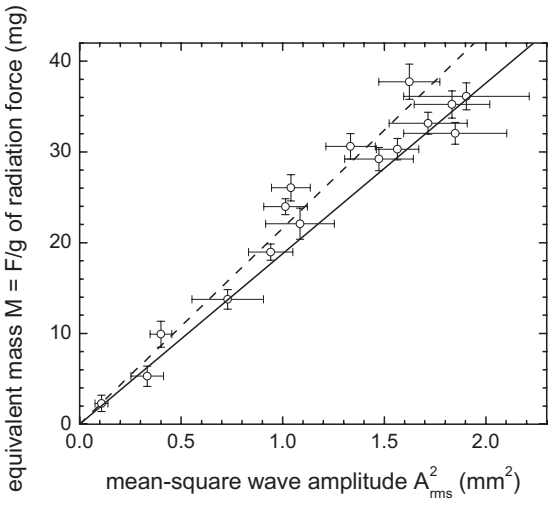


Fig. 6. Equivalent mass $F/g$ of the radiation force $F$ on a plate as a function of the mean-square vertical displacement $A^2_{rms}$ of the surface waves. The points are experimental, and the solid line is the gravity wave theory. The dashed line is a rough approximation for gravity-capillary waves. The theory lines have no adjustable parameters.

Further attempts to understand the deviation led us to question our assumption that the effect of surface tension is negligible. The radiation force due to a monofrequency gravity-capillary wave is known.[21] The surface tension causes a frequency dependence, which complicates the analysis of the force for random waves. We show in the Appendix that an approximation of the force for a peaked spectrum can be readily determined. The result in our case is that the force due to gravity-capillary waves is related to the pure gravity wave force by an $\approx$15% increase in the slope of the solid line in Fig. 6. The new (dashed) line indicates that surface tension is responsible for the systematic deviation of the experimental data from the pure gravity wave theory.

Finally, we consider a possible repulsive force between the plates, which is expected due to the acoustic analog of the Casimir effect. As the plate separation distance is increased for a fixed frequency band of waves, a small repulsive force should occur when the plates are separated by approximately a half-wavelength corresponding to the minimum frequency.[5] We performed a visual search for the repulsion, increasing the equilibrium plate separation in increments of 0.25 cm. The attractive force eventually decreases to approximately zero, or a possible small repulsive force, at a plate separation distance of 4.25 cm. For greater separation distances, the force is weakly attractive. This minimum in the force indicates that a more refined search could conclusively yield a repulsion force. Our minimum wave frequency of 6.0 Hz (Fig. 5) corresponds to a wavelength of 4.5 cm (Fig. 2), and thus the repulsive force should occur for a half-wavelength plate spacing of 2.3 cm rather than the observed value of 4.25 cm. The discrepancy could be due to the difference between acoustics and water waves. Another possibility is that the discrepancy is a finite-size container effect due to the width of our plates (9.5 cm) not being small compared to the diameter of the dish (19 cm), which could inhibit waves from entering at the openings of the plates.

## VII. CONCLUDING REMARKS

Casimir-type effects occur, in general, for two bodies in a homogeneous and isotropic spectrum of any kind of random waves that carry momentum. A net attractive force occurs between two parallel plates in the typical case where the radiation force is reduced between them. We have described a system of plates suspended in a dish of parametrically driven liquid surface waves, which offers a visual demonstration of an analog Casimir effect. We have derived the force due to gravity waves for the case where the waves are negligible between the plates, and have shown that this force can be substantial for two side-by-side ships in a rough sea. Our measurements are in approximate agreement with the theory. The observed systematic error is consistent with our approximation of the effect of surface tension. At greater plate separation distances such that waves occur between the plates, we observe an indication of a repulsive force.

We have taken only a first step in quantifying the water wave analog of the Casimir effect. The situation in which waves exist both outside and between the plates could be analyzed and is expected to yield a repulsive force for some conditions. A related problem is to quantify the force between two side-by-side ships in a rough sea as a function of wavelength. A careful experimental search for the expected repulsive force could be done. Possible improvements to the apparatus include direct rather than parametric excitation of

the waves, which would substantially reduce the large fluctuations of amplitude. Rigid pendulums could be constructed with lightweight rods that are pivoted with very low friction V-jewel bearings, similar to an acoustic radiometer.[9] This restriction of the motion of a plate to one degree of freedom would allow much quicker measurements of the displacement with an ultrasonic ranger, optical ranger, or rotary encoder. There is also the issue of possible finite-size container effects. A larger container could be used with a large loudspeaker that is adapted for use as a shaker if parametric excitation is used. Finally, surface tension could be completely incorporated into the analysis of the data.

## APPENDIX: APPROXIMATE THEORETICAL FORCE DUE TO RANDOM GRAVITY-CAPILLARY WAVES

The dispersion relation (1) for gravity-capillary waves can be expressed as $\omega^2 = gk(1+B)$, where the effect of surface tension is given by the dimensionless *Bond number* $B = \gamma k^2/\rho g$.[21] We conveniently express the Bond number in terms of the crossover wavelength in Eq. (2) as $B = (\lambda_c/\lambda)^2$, where $\lambda_c = 1.07$ cm for ethyl alcohol. From Fig. 5 the wave spectrum is a maximum at 8.0 Hz, which corresponds to $\lambda = 2.8$ cm according to Fig. 2. The Bond number at the peak is $B_p = 0.15$. That this value is not very small compared to unity indicates that surface tension may not be negligible for our experiment.

The effect of surface tension in the radiation force of a monofrequency wave is to multiply the pure gravity wave force by the factor $1+B$.[21] From Eq. (5) the radiation force for a spectrum of waves is then

$$F = \frac{1}{4}\rho g a \int [1 + B(\omega)] A_\omega^2 d\omega. \tag{A1}$$

Surface tension causes a frequency dependence which substantially complicates the analysis of experimental data. An approximate value of the force is readily obtained by evaluating $B(\omega)$ at the peak, which yields

$$F = \frac{1}{4}\rho g a (1 + B_p) \int A_\omega^2 d\omega = \frac{1}{4}\rho g a (1 + B_p) A_{\mathrm{rms}}^2. \tag{A2}$$

Compared to the pure gravity wave result (5), the effect of surface tension is to increase the slope of the line of $F/g$ versus $A_{\mathrm{rms}}^2$ by approximately the factor $1+B_p = 1.15$. This approximation corresponds to the dashed line in Fig. 6.

[a]Electronic mail: denardo@nps.edu


[1] S. K. Lamoreaux, "Resource Letter CF-1: Casimir force," Am. J. Phys. **67**, 850–861 (1999).

[2] P. W. Milonni, R. J. Cook, and M. E. Goggin, "Radiation pressure from the vacuum: Physical interpretation of the Casimir force," Phys. Rev. A **38**, 1621–1623 (1988).

[3] E. Elizalde and A. Romeo, "Essentials of the Casimir effect and its computation," Am. J. Phys. **59**, 711–719 (1991).

[4] S. L. Boersma, "A maritime analogy of the Casimir effect," Am. J. Phys. **64**, 539–541 (1996).

[5] Andrés Larraza and Bruce Denardo, "An acoustic Casimir effect," Phys. Lett. A **248**, 151–155 (1998); Andrés Larraza, Christopher D. Holmes, Robert T. Susbilla, and Bruce Denardo, "The force between two parallel rigid plates due to the radiation pressure of broadband noise: An acoustic Casimir effect," J. Acoust. Soc. Am. **103**, 2267–2272 (1998).

[6] A. Larraza, "A demonstration apparatus for an acoustic analog to the Casimir effect," Am. J. Phys. **67**, 1028–1030 (1999).

[7] D. J. Griffiths and E. Ho, "Classical Casimir effect for beads on a string," Am. J. Phys. **69**, 1173–1176 (2001).

[8] S. Ref. 1 and also James H. Cooke, "Casimir force on a loaded string," Am. J. Phys. **66**, 569–572 (1998).

[9] B. Denardo and T. G. Simmons, "An acoustic radiometer," Am. J. Phys. **72**, 843–845 (2004).

[10] Timothy H. Boyer, "Casimir forces and boundary conditions in one dimension: Attraction, repulsion, Planck spectrum, and entropy," Am. J. Phys. **71**, 990–998 (2003); V. Hushwater, "Repulsive Casimir force as a result of vacuum radiation pressure," *ibid.* **65**, 381–384 (1997).

[11] Pasco Scientific <www.pasco.com>, pendulum clamp, model SE-9443.

[12] Corning Pyrex <www.corning.com>, Lowell, MA, crystallizing dish, model 3140–190.

[13] APS Acoustic Power Systems, Dynamics <www.navcon.com>, shaker, model 120, and power amplifier, model 114.

[14] B. Denardo, W. Wright, and S. Putterman, "Observation of a kink soliton on the surface of a liquid," Phys. Rev. Lett. **64**, 1518–1521 (1990).

[15] L. D. Landau and E. M. Lifshitz, *Mechanics*, 3rd ed. (Pergamon, New York, 1976), pp. 80–84.

[16] Stanford Research Systems <www.thinksrs.com>, high pass/low pass 115 dB per octave ("brick-wall") filter, model SR650.

[17] L. D. Landau and E. M. Lifshitz, *Fluid Mechanics* (Pergamon, New York, 1959), Secs. 12 and 61.

[18] G. B. Whitham, *Linear and Nonlinear Waves* (Wiley, New York, 1974), pp. 553–563.

[19] The wave height probe is briefly mentioned in Junru Wu and Isadore Rudnick, "Amplitude-dependent properties of a hydrodynamic soliton," Phys. Rev. Lett. **55**, 204–207 (1985); Junru Wu, Robert Keolian, and Isadore Rudnick, "Observation of a nonpropagating hydrodynamic soliton," *ibid.* **52**, 1421–1424 (1984). The probe is also mentioned in Ref. 14.

[20] Stanford Research Systems, lock-in amplifier, model SR850.

[21] Paul H. LeBlond and Lawrence A. Mysak, *Waves in the Ocean* (Elsevier, New York, 1978), Secs. 11 and 13.